Incorporating Prior Knowledge in Local Parametric Modeling for Frequency Response Measurements

Document license:
TAVERNE

Document status and date:
Published: 01/01/2022

Document Version:
Publisher's PDF, also known as Version of Record (includes final page, issue and volume numbers)

Please check the document version of this publication:

• A submitted manuscript is the version of the article upon submission and before peer-review. There can be important differences between the submitted version and the official published version of record. People interested in the research are advised to contact the author for the final version of the publication, or visit the DOI to the publisher's website.
• The final author version and the galley proof are versions of the publication after peer review.
• The final published version features the final layout of the paper including the volume, issue and page numbers.
Link to publication

Incorporating Prior Knowledge in Local Parametric Modeling for Frequency Response Measurements: Applied to Thermal/Mechanical Systems

Enzo Evers [ID], Bram de Jager [ID], and Tom Oomen [ID], *Senior Member, IEEE*

Abstract—**Frequency response function (FRF) identification is a key step in experimental modeling of many applications, including mechatronic systems. Applying these techniques to systems where measurement time is limited leads to a situation where the accuracy of the identified model is deteriorated by transient dynamics. This article aims to develop an identification procedure that mitigates these transient dynamics by employing local parametric modeling techniques. To improve the modeling accuracy, prior knowledge is suitably incorporated in the procedure while at the same time allowing for rational parameterizations that maintain a closed-form solution. The prior knowledge is exploited in a relevant local frequency range using a specific Möbius transformation. Preexisting methods, including the commonly used local polynomial method, are recovered as a special case. The presented framework leads to accurate identification results in a simulation study as well as on experimental measurement data.**

Index Terms—**Frequency response function (FRF), precision mechatronics, system identification, thermomechanical.**

I. INTRODUCTION

FREQUENCY response function (FRF) identification is a key step in identification and control. Acquiring FRFs is often fast, inexpensive, and accurate and requires very limited user intervention. The obtained FRFs are used for many purposes, ranging from controller design by manual tuning [1], optimal synthesis [2], stability analysis, and interaction analysis [3] to parametric identification [4]. Also, these FRFs are used in many application domains, e.g., in mechanical systems with flexible dynamics [5], [6], thermal systems [7], electrical systems [8], and combustion systems [9].

Identification of FRFs has recently been substantially advanced by explicitly mitigating transient errors. Indeed, one of the tacit assumptions is that the system under test

is in steady state, which is often not valid for experimental systems. Moreover, due to the slow dynamics in certain applications, e.g., thermal–mechanical systems, transients are increasingly relevant. In the local polynomial method (LPM) [10], the smoothness, in the frequency domain, of the transient response is exploited by locally approximating the transfer function by a polynomial function to estimate and remove the transient component. In [11], this is generalized toward the local rational method (LRM), which uses a rational function in the local approximation.

Although the general parameterization used in the LRM enables improved identification results, the LRM involves an optimization problem that introduces additional challenges. As a key advantage, the LRM is a more general parameterization, directly recovering the LPM as a special case, and the additional freedom in the parameterization allows to capture dynamics, especially lightly damped, more accurately (see [12] for a theoretical analysis of the local approximation error and [5] for experimental evidence). On the other hand, the rational parameterization leads to a nonconvex optimization problem, which is approximated in typical LRM approaches as in [13]. Further improvements to employ an iterative algorithm have mixed outcomes (see [5]). Furthermore, as a direct consequence, the variance results, which are valid for LPM, are only accurate for the LRM for sufficiently high signal-to-noise ratio (SNR) due to a bias effect.

This article aims to present a unified framework for FRF identification that employs a rational local parameterization, in conjunction with a closed-form optimizer to yield reliable variance expressions and improved estimation accuracy. This is achieved by exploiting prior knowledge on the system, characterized by pole locations in the complex plane, e.g., resonance frequency region in mechanical systems [5], or pole locations on the real axis [14], [15] for thermal systems.

In [16], VF is used to provide the local rational parameterization with estimated pole locations. The VF algorithm is adapted to work on transient input–output data and employs an iterative process to estimate the pole locations. In [17], a bootstrapped total least squares (LS) estimator is employed to obtain unbiased estimates for a local rational model.

The approach in this article exploits the freedom of selecting those poles at a prescribed location. The presented approach is linear in the parameters, similar to the LPM, and therefore maintains the associated benefits, e.g., an analytical solution
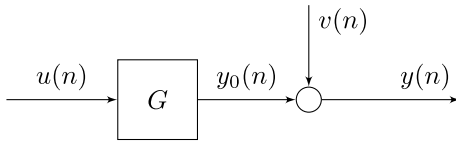
Fig. 1. Discrete-time LTI system in an open-loop setting with input $u(n)$, measurement noise $v(n)$, and output $y(n)$.

and bias and variance expression. The approach utilizes orthonormal rational basis functions (OBFs), which are well studied [18]–[20] to form the basis for the local regression problem. Moreover, it is shown that it requires the development of OBFs with complex coefficients over the real line, which is in sharp contrast to the typical use of OBFs in system identification, where the support is typically over the imaginary axis or the unit disk. Indeed, local parametric methods (LPM/LRM) often tacitly represent FRFs of systems by complex-valued transfer functions that are evaluated over the real axis.

The main contributions of this article are given in the following.

C1: A local parametric method is developed that uses a linearly parameterized basis, leading to an efficient optimization and closed-form solution, providing an accurate variance analysis yielding a reliable quality metric and exploiting prior knowledge.

C2: Development of the necessary theory of OBFs using single complex pole parameterizations over the real line and transformation of prior knowledge to this domain.

C3: Validation of the method by application on relevant systems, e.g., on resonant dynamics in a simulation study of a mechanical system and first-order dynamics in an experimental study on a high-tech industrial thermal setup.

This article is organized as follows. In Section II, FRF identification under transient conditions is investigated. In Section III, the local parametric method using the general parameterization considered is presented. In Section IV, a design for the local approximation basis is introduced together with a framework for orthonormal rational functions on the real line. A Möbius transformation is used to connect different components of the framework to appropriate prior knowledge and previous results. In Section V, the method is applied in a case study on relevant industrial applications, involving a simulation study involving lightly damped resonant dynamics and experiments on a high-tech industrial thermal setup. In Section VII, conclusions are presented.

II. PROBLEM FORMULATION

A. Transients in FRF Identification

In this section, the role of transients in FRF identification is investigated.

Consider a discrete-time linear time-invariant (LTI) single-input–single-output (SISO) system G in an open-loop setting, as shown in Fig. 1, and an excitation input $u(n)$. Then, the output $y(n)$, for an infinite time interval $n \in (-\infty, \infty)$,

is given by

$$y(n) = \sum_{k=-\infty}^{\infty} u(k)g(n-k) + v(n) \qquad (1)$$

where $g(n)$ is the impulse response of G and $v(n)$ is the noise contribution on the output. By applying the discrete Fourier transform (DFT)

$$X(k) = \frac{1}{\sqrt{N}} \sum_{n=0}^{N-1} x(n)e^{\frac{-i2\pi kn}{N}} \qquad (2)$$

on a finite interval, i.e., $n \in \{0, 1, \ldots, N-1\}$ of (1), it yields

$$Y(k) = G(\Omega_k)U(k) + T(\Omega_k) + V(k) \qquad (3)$$

in the frequency domain, where $G(\Omega_k)$ is the FRF of the dynamic system. Also, $Y(k)$, $U(k)$, and $V(k)$ are the DFT of $y(n)$, $u(n)$, and $v(n)$, respectively. Here, Ω_k denotes a generalized frequency unit, e.g., in continuous time $\Omega_k = j\omega$ and in discrete time $\Omega_k = e^{j\omega_k T_s}$, where T_s is the sample time and k denotes the kth frequency bin, and the latter is used throughout.

In (3), $T(\Omega_k)$ accounts for the transients for both the system response $T_G(\Omega_k)$ and the noise $T_V(\Omega_k)$. The transient terms are directly related to the initial and final conditions of the system, i.e., the transition of an infinite to a finite interval such that the relation (3) is an exact representation. Also, the estimation error by neglecting the term $T(\Omega_k)$ is often referred to as leakage error [4]. An insightful interpretation (see also [11]) of $T(\Omega_k)$ can be made by using a state-space realization of the system G in Fig. 1, e.g.,

$$x(n+1) = Ax(n) + Bu(n)$$
$$y(n) = Cx(n) + Du(n) + v(n) \qquad (4)$$

where $x(n) \in \mathbb{R}^{n_x}$ is the state vector with n_x the number of states. By then applying the DFT to (4), this directly connects to (3) through

$$G(\Omega_k) = C(e^{j\omega_k}I - A)^{-1}B + D \qquad (5)$$
$$T(\Omega_k) = C(e^{j\omega_k}I - A)^{-1}(x(0) - x(N))e^{j\omega_k} \qquad (6)$$

where $G(\Omega_k)$ is the FRF of the LTI system and $T(\Omega_k)$ is the transient contribution in the frequency domain. This shows that $T(\Omega_k)$ and $G(\Omega_k)$ exhibit similar but not identical dynamics since they share the same poles and it is assumed that no pole/zero cancellations are present. However, the zeros of their transfer functions can be different.

B. Classical Approach

The finite-time response in (3) contains the additional terms $T(\Omega_k)$ and $V(k)$. A classical approach to identify the system $G(\Omega_k)$ is to use the empirical transfer function estimate (ETFE), i.e.,

$$\hat{G}(k) = Y(k)U^{-1}(k). \qquad (7)$$

Analysis reveals that

$$G(\Omega_k) - \hat{G}(k) = \underbrace{T(\Omega_k)(k)U^{-1}(k) + V(k)U^{-1}(k)}_{\text{estimation error}}. \qquad (8)$$

Hence, the transients, in addition to the noise contribution $V(k)$, lead to an estimation error.
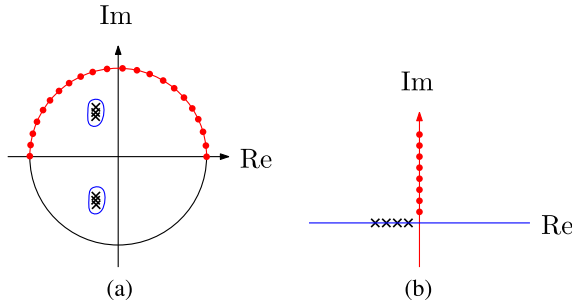
Fig. 2. Examples of prior knowledge in different domains and applications. (a) Prior in discrete time, where $\Omega_k = e^{j\omega_k}$ (●), mechanical applications, where a frequency region or damping coefficient (——) of the resonance mode is approximately known. (b) Prior in continuous time, where $\Omega_k = j\omega_k$ (●), thermal applications, where the poles lie on the real axis (——).

C. Transients in Different Applications

The result (8) reveals that transients lead to estimation errors of the true system $G(\Omega_k)$. From (5) and (6), the system dynamics, i.e., pole locations, largely determine the transient contribution.

The central idea in this article is that the application domain provides clear prior knowledge on the locations of these poles. In Fig. 2, pole locations are shown for a mechanical system, in Fig. 2(a), and a thermal system, in Fig. 2(b). An *ad hoc* solution that is often employed to cope with transient data is to remove the initial transient response from the identification data. Electromechanical systems, e.g., servo-positioning systems, often have lightly damped dynamics and small time constants. For these systems, the transient contribution in (3) can sometimes be substantial due to low damping. For other systems, e.g., thermomechanical systems [21], the time constants are significantly larger and the transient contributions constitute a dominant part of the output response. Waiting for the initial transient to settle requires an unacceptable increase in experiment time. FRF identification for a more general class of systems, e.g., including thermomechanical systems, requires a method capable of coping with data obtained under transient conditions.

In this article, an approach that explicitly considers the transient term $T(\Omega_k)$ to obtain an unbiased estimate of $G(\Omega_k)$ is presented. This eliminates the need to discard the initial transient data, thus achieving significant savings in the necessary experiment time to accurately identify the system.

D. Problem Formulation

The problem considered in this article is as follows. Given an input–output sequence, u and y where y contains a transient response, provide an accurate nonparametric FRF estimate $\hat{G}(\omega)$ of the true system $G_0(\omega)$ accompanied with a reliable variance estimation $\hat{C}_v(\omega)$.

To address this, a new parameterization is employed, which allows for the estimation of transient responses by solving an optimization problem that has a closed-form solution, thereby providing an accurate estimate and accompanying variance expressions. Moreover, this method facilitates the incorporation of appropriate prior knowledge, enabling increased estimation accuracy.

III. LOCAL PARAMETRIC MODELING

In this section, a local parametric approach is presented with a rational parameterization that allows convex optimization, in particular a closed-form solution, leading to contribution $C1$. The outline of the section is as follows. First, the concept of local parametric modeling is presented. Second, the linear parameterization used in this article is presented. Third, the presented approach is connected to previous results on local parametric modeling, including the LPM [4] and the LRM [11]. In fact, these results are recovered as special cases.

A. Local Modeling

Local parametric methods construct approximations of $G(e^{i\omega_k})$ and $T(e^{i\omega_k})$ in (3) on a subset of points

$$\lambda = \{k - l, \dots, k + l\} \subset \mathbb{N} \tag{9}$$

i.e., a local window of width $2l+1$ with $l \in \mathbb{N}$, in the complex plane. This is shown in Fig. 3 where the first- and second-order local approximations are shown.

Remark 1: Throughout this article, the notation $\{k - l, \dots, k + l\}$ is dropped, and k indicates a single DFT-bin and λ indicates the local window, i.e., $\lambda = \{k - l, \dots, k + l\} \subset \mathbb{R}$.

The key mechanism underlying local parametric methods is the smoothness of both $G(\Omega_k)$ and $T(\Omega_k)$ in (3).

In particular, the input $U(k)$ is selected such that it is sufficiently exciting and "wild," i.e., having a nonsparse and nonsmooth frequency spectrum in magnitude and/or phase. Signals that are particularly suited are (filtered) white noise or random-phase multisines. This ensures that $G(\Omega_k)$ can be distinguished from $T(\Omega_k)$ since the latter is not affected by the system input $U(k)$. For each frequency point k, a local parametric approximation is constructed over neighboring points λ, e.g., by polynomial functions in the LPM and rational functions in the LRM. Then, an estimate for the transient component at $T(\Omega_k)$ is constructed using this local approximation such that it can subsequently be removed from $G(\Omega_k)$. This is shown in Fig. 3 for $G(k)$. The result for the transient $T(k)$ follows along conceptually similar lines (for more details on the local parametric method in general, see [21], [22]). In the remainder of this article, the emphasis lies on constructing a suitable local parametric approximation basis for the functions $G(\Omega_k)$ and $T(\Omega_k)$.

Remark 2: The local modeling approach presented in this article is still classified as a nonparametric identification approach. The local parametric models are solely used as an intermediate step to obtain the FRM at a single frequency point k, after which they are discarded.

B. Linearly Parameterized Rational Parameterization

Consider again (3) and let

$$G(\Omega_\lambda) = \sum_{b=0}^{N_b} \theta_G^k(b) \Psi(b, \lambda) \tag{10}$$

$$T(\Omega_\lambda) = \sum_{b=0}^{N_b} \theta_T^k(b) \Psi(b, \lambda) \tag{11}$$
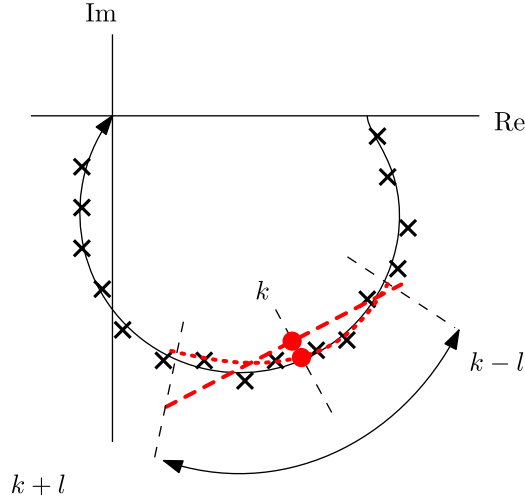
Fig. 3.   Resulting local approximation of $G(\Omega_k)$ in local parametric modeling in the complex plane. Here, a first-order (- -) and second-order (....) approximation of the true plant (——) is constructed using the measured data ($\times$) in the local window λ yielding an estimate for $G(\Omega_k)$ at k ($\bullet$). The local approximation for $T(\Omega_k)$ follows along conceptually similar lines.

such that locally the terms in (3) are approximated in a window λ by an expansion of degree N_b using general basis functions $\Psi(b, \lambda) \in \mathbb{C}$, where $\theta_G^k(b) \in \mathbb{C}$ and $\theta_T^k(b) \in \mathbb{C}$ are the local coefficients for $G(\Omega_\lambda)$ and $T(\Omega_\lambda)$, respectively. Note that $\Psi = \lambda^b$ in (10) for the well-known LPM. For each point k, this local approximation yields

$$\hat{Y}(\lambda) = \underbrace{\begin{bmatrix} \theta_G(k) \; \theta_T(k) \end{bmatrix}}_{\Theta(k)} \underbrace{\begin{bmatrix} \Psi(\lambda) \otimes U(\lambda) \\ \Psi(\lambda) \end{bmatrix}}_{K(U(\lambda), \Psi(\lambda))} \tag{12}$$

where $\Theta(k)$ contains the local approximation coefficients for the basis functions contained in the regression matrix $K(\lambda) = K(U(\lambda), \Psi(\lambda))$. From this local approximation, only the center value, i.e., $G(\Omega_k)$ is used, as shown in Fig. 3. This local approximation is repeated to obtain an estimate of $G(\Omega_k)$ and $T(\Omega_k)$ for each frequency bin k.

Remark 3: The input $U(\lambda)$ is assumed to vary sufficiently over the full input spectrum such that $G(\Omega_\lambda)U(\lambda)$ can be distinguished from $T(\Omega_\lambda)$ so $K(\lambda)$ does not lose rank, i.e., the input is sufficiently "wild." This can be achieved by, e.g., broadband noise excitation or random-phase multisines [4]. The coefficients $\Theta(k)$ are found by solving the LS problem

$$\hat{\Theta}(k) := \arg \min_{\Theta} \sum_{p=k-l}^{k+l} |Y(p) - \Theta(k)K(p)|^2 \tag{13}$$

which should be overdetermined. Then, $\hat{\Theta}$ is given by

$$\hat{\Theta}(k) = Y(\lambda)K(\lambda)^H (K(\lambda)K(\lambda)^H)^{-1} \tag{14}$$

where $K(\lambda)^H$ is the Hermitian transpose of the regression matrix $K(\lambda)$ in (12). Due to the closed-form solution, which resembles the LPM [4, Sec. 7.2.2], an estimate for the noise covariance matrix is given by

$$\hat{C}_v(k) = \frac{1}{q}(Y(\lambda) - \hat{Y}(\lambda))(Y(\lambda) - \hat{Y}(\lambda))^H \tag{15}$$

where q is the degree of freedom of the residual $Y(\lambda) - \hat{Y}(\lambda)$, i.e., $q = 2l + 1 - 2(N_b + 1)$. The final covariance on the estimated FRF $\text{Cov}(\text{vec}(\hat{G}(k)))$ is then determined by an appropriate transformation, e.g., [4, Ch. 7].

Indeed, the covariance of the estimated FRF is given by

$$\text{cov}(\text{vec}(\hat{G}(k))) = \overline{S^H S} \otimes \hat{C}_v(k) \tag{16}$$

where

$$S = K(\lambda)^H (K(\lambda)K(\lambda)^H)^{-1} \begin{bmatrix} I_{n_u} \\ 0 \end{bmatrix} \Psi(k) \tag{17}$$

and vec() denotes a stacking of the columns of the matrix and n_u is the number of inputs of the estimated system.

Remark 4: The key point is that (15) holds for a linearly parameterized model (10), which is in sharp contrast to the LRM (see Section III-C), in which case variance estimations are typically biased. This is caused by the Levy approximation that introduced measurement data in the regressor matrix. The result (15) and (16) holds for any linearly parameterized basis, and the results in [4] are recovered as a special case.

The basis Ψ is general and allows for user-chosen parameterizations. For instance, the basis Ψ can be chosen to be a polynomial, rational, or fractional function of the window parameter λ. In Section II-C, it is shown how earlier approaches fit in the framework. Then, a new approach is presented, which enables the incorporation of prior knowledge.

C. Connection to LRM

A particular choice regarding the parameterization in (10) is to select rational polynomials for Ψ, which directly connects to previously used rational functions in the LRM [11]. To introduce the LRM, consider the optimization problem

$$\hat{\Theta}_{\text{LRM}} := \arg \min_{\Theta_{\text{LRM}}} \sum_{p=k-n}^{k+n} \left| Y(p) - \frac{N_\lambda}{D_\lambda} U(p) - \frac{M_\lambda}{D_\lambda} \right|^2 \tag{18}$$

where

$$N_\lambda = \sum_{s=0}^{N_n} n_s(k)\lambda^s \tag{19}$$

$$M_\lambda = \sum_{s=0}^{N_m} m_s(k)\lambda^s \tag{20}$$

$$D_\lambda = 1 + \sum_{s=1}^{N_d} d_s(k)\lambda^s. \tag{21}$$

In case of the typical LRM parameterization, the free parameters are $\Theta_{\text{LRM}} = [n_0, \ldots, n_{N_m}, m_0, \ldots, m_{N_m}, d_1, \ldots, d_{N_d}] \in \mathbb{C}^{N_n + N_m + N_d}$, where N_n, N_m, and N_d denote the order of the plant and transient numerator and common denominator, respectively. From (18), the LPM is directly recovered by setting $[d_{N_d} \; \cdots \; d_1] = 0$. For general D_w, (18) is nonlinear in the parameters, and generally, no closed-form solution similar to (14) exists. At least two approaches [11], [12], [23], [24] have been pursued to determine (18) and find Θ_{LRM}: 1) iteratively solving the LS problem, which has been applied in [23] with mixed results or 2) multiplying the criterion with D_w as in the classical approach in [13], which introduces an

a priori unknown weighting function in (18). On top of these aspects, both approaches lead to a situation where K contains measurement data that are corrupted with noise, potentially introducing errors in the variance estimate (15) and (16) (see also Remark 4). The form in (12) combines a general rational basis with the benefits associated with a linear parametrization where the regression matrix is noise-free.

In this article, an approach is presented based on orthogonal basis functions that enable the incorporation of prior knowledge. Orthogonality enables a systematic way to build the basis in a numerically reliable way. By using an appropriate Möbius transformation, both the basis can be transformed from different circles or lines in the complex plane, as well as the prior knowledge. Specific choices of the prior knowledge lead to the LPM, which is a clear result. The LRM essentially relates directly to specific choices of poles, while in many cases, it is found by solving a related identification problem by writing it as an equation error problem.

IV. LRMP

The local parametric approach in Section III yields improved FRF estimation by explicitly taking transient contributions into account. For this, a local parametric parameterization is used to approximate $T(\Omega_k)$ as a linear combination of basis functions Ψ. In this section, an approach facilitating the construction of a suitable basis Ψ is presented, henceforth referred to as the LRM with prescribed poles (LRMP).

A. Approximation Basis

In this section, the parameterization (10) is considered where the key idea is to select a basis Ψ such that the closed-form expression to (13) is retained. Consider a basis Ψ composed of rational functions with single complex poles, i.e.,

$$\Psi(\omega) = \sum_{b=0}^{N_b} \frac{1}{\omega + \beta_b} \quad (22)$$

where $\beta_b \in \mathbb{C}, b \in 1, \ldots, n_b$ are the prescribed poles of the rational functions and $\omega \in \mathbb{R}$ is the (local) frequency parameter on the real line. In Section V, it is illustrated how this parameter β_k can be connected to discrete- or continuous-time system poles. This basis facilitates the modeling of resonant behavior and offers a general parameterization, while (10) remains linear in the parameters. For the local approximation (10), the basis functions coefficients may be complex; indeed, such model structures with complex parameters are standard in the local methods. In previous methods, e.g., in the LPM, the poles of the basis functions are all placed at ∞. In this article, the freedom in the location of the prescribed poles in (22) is exploited to obtain a higher approximation accuracy by including prior knowledge. In Section V-A, the transformation, to the $\omega \in \mathbb{R}$ domain, of this prior knowledge is investigated further using an appropriate Möbius transformation.

Provided that the poles β_b have been selected (see also Section V), the basis can be systematically constructed using orthogonal rational functions on the real line. These rational functions are a result of Gram–Schmidt orthogonalization of the basis in (22).

Theorem 1: Given $\beta_b \in \mathbb{C}$ where $b \in [0, N_b]$, i.e., the poles in (22). Let $\Psi(\omega)$ be parameterized as

$$\Psi_b(\omega) = \begin{cases} \sqrt{-2\mathrm{Im}(\beta_0)}\dfrac{-j}{\omega + \beta_0} & b = 0 \\[2mm] \sqrt{-2\mathrm{Im}(\beta_b)}\dfrac{-j}{\omega + \beta_b}\prod_{l=0}^{b-1}\dfrac{\omega + \bar{\beta}_l}{\omega + \beta_l} & b \neq 0 \end{cases} \quad (23)$$

and then

$$\frac{1}{2\pi}\int_{-\infty}^{+\infty}\Psi_n(\omega)\overline{\Psi_m}(\omega)d\omega = \begin{cases} 1, & n = m \\ 0, & n \neq m \end{cases} \quad (24)$$

where $\omega \in \mathbb{R}$, i.e., the basis Ψ is orthonormal on the real line. A proof of Theorem 1 is provided in the Appendix. The basis in Theorem 1 is novel since the orthonormal basis functions are considered on the real line, opposed to on the imaginary line.

The orthogonality of the functions Ψ facilitates the repetition of poles to expand the basis, improving the approximation of the true FRF [25]. In fact, for a function $f(\omega)$ in the Hardy space H_2 for arbitrary $\epsilon > 0$ and for sufficiently large m, an element $g(\omega) \in \{\Psi_b(\omega)\}_{k=1}^{m}$ can be found such that $||f - g||_2 \leq \epsilon$, i.e., the basis $\Psi(\omega)$ is complete in H_2. The basis Ψ is complete if the following theorem holds.

Theorem 2: The model set spanned by the basis functions $\{\Psi_b(\omega)\}_{n \geq 0}$ is complete in all of the spaces $H_p, 1 < p < \infty$ if and only if

$$\sum_{k=1}^{\infty}\frac{-\mathrm{Im}\{\beta_b\}}{1 + |\beta_b|^2} = \infty. \quad (25)$$

A proof for this is presented in the Appendix.
The condition (25) in Theorem 2 is mild and fulfilled by (23) if the poles β_b are not on the real line. Finally, the orthogonality of the basis potentially yields improved numerical conditioning for the approximation problem [26].

Remark 5: The basis in Theorem 1 is orthogonal when evaluated over the real line as in (24). In the local window λ, this orthogonality can be lost since a discrete set of points is considered that no longer spans the complete real line. A solution for this could be found in line with [27] that considers a discrete data-dependent basis to improve conditioning. The conditioning [28] of (23) improves with the window size for $\lim_{\lambda \to N}$, where N is the total amount of samples in a measurement.

V. EMPLOYING PRIOR KNOWLEDGE: MÖBIUS TRANSFORMATION

In this section, it is shown how to incorporate prior knowledge from different domains using a specific Möbius transformation, constituting contribution C2. Moreover, this transformation is used to connect the presented framework to previous results from the literature.

A Möbius transformation is a conformal mapping defined on the extended complex plane $\mathbb{C}_\infty = \mathbb{C} \cup \{\infty\}$ of the form

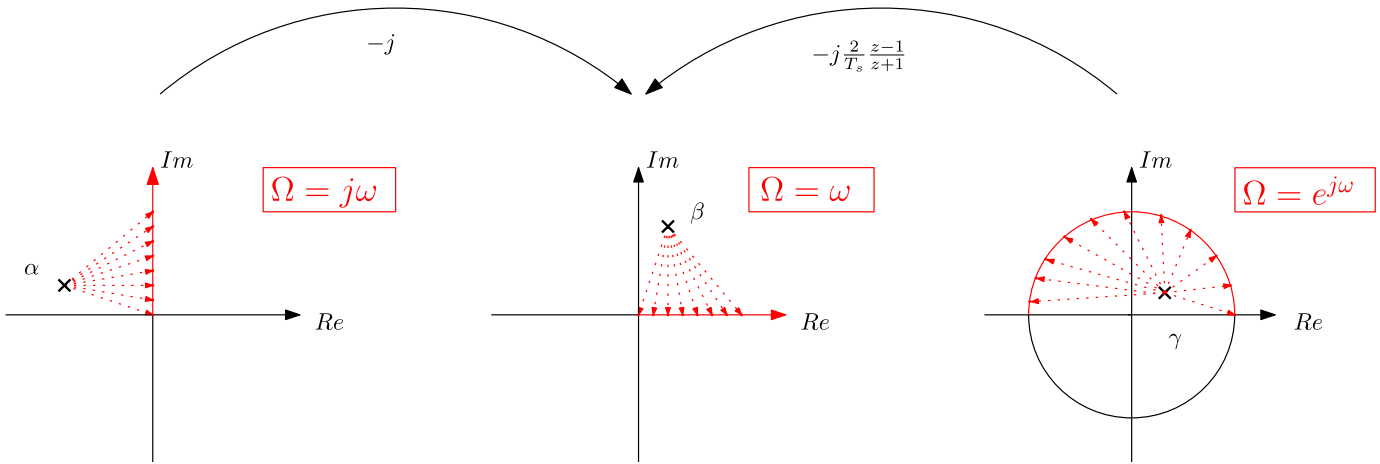$$f(z) = \frac{az + b}{cz + d} \quad (26)$$

Fig. 4. Complex plane, with a pole location β as a function of $\Omega = \omega$, a pole location α as a function of $\Omega = j\omega$, or a pole location γ as a function of $\Omega = e^{j\omega}$. By applying the required Möbius transformations, pole locations in different domains can be incorporated in the proposed parameterization.

where $z \in \mathbb{C}_\infty$ and $a, b, c, d \in \mathbb{C}$ satisfy $ad - bc \neq 0$. A well-known special case of this transformation is the bilinear transform, i.e., Tustin's method [29].

Remark 6: In previous local parametric modeling methods, discrete-time frequency-domain data, i.e., an FRF evaluated on points on the unit disk $e^{j\omega}$, is approximated by local models that are a function of $k \in \mathbb{N}$ on the real line, i.e., the DFT bins, as shown in Fig. 3. The transformation from $s = j\omega$ or $z = e^{j\omega}$ to the ω domain is often implicit, but it is essential when including prior system knowledge, as is done in this article.

A. Prior Knowledge

In Section IV, a suitable basis Ψ for the local approximation (10) is presented, i.e., (23), where β_i is selected *a priori*. However, prior knowledge, e.g., system poles, is often defined in terms of the Laplace variable s or the Z transform variable z, where the frequency response is obtained by substituting $s = j\omega$ and $z = e^{j\omega}$, respectively. In contrast, the functions (22) for which the poles are defined as β are evaluated on the real line w. Consequently, prior knowledge regarding the poles of the physical system $G(\Omega_k)$ cannot directly be incorporated in the local function (22). The appropriate prescribed poles β for (23) are transformed using the forthcoming results from prior knowledge in the continuous domain α or discrete domain γ, by employing the Möbius transformations shown in Fig. 4.

a) Continuous Time α: Given some knowledge on the system poles in continuous time domain, i.e., $\Omega_k = s$, an equivalent prior is obtained for the ω domain by using $\beta = -j\alpha$ such that their FRF is equal, e.g., $\Psi(\beta)|_\omega \equiv G(\alpha)|_{j\omega}$.

b) Discrete Time γ: In the discrete-time domain $\Omega_k = z$, a similar approach is applied by mapping the pole locations using a bilinear transformation $\beta = -j(2/T_s)(z - 1/z + 1)\gamma$ that is known as a Cayley transformation. However, care has to be taken since, for $\Psi(\beta)|_\omega \equiv G(\gamma)|_{e^{j\bar{\omega}T}}$, it holds that $\omega \neq \bar{\omega}$, i.e., the frequency $\bar{\omega}$ is distorted with respect to the original frequency ω. If aliasing is particularly relevant, a future

extension may be to use the impulse invariant transformation in favor of the bilinear transform.

Remark 7: To compensate for the frequency distortion when including discrete-time domain prior knowledge, several approaches can be used. First, the warping can be ignored as is commonly done in LPM techniques for discrete-time systems. This could be used if the prior knowledge is mainly located at lower frequencies, where $\omega \approx \bar{\omega}$. Second, prewarping in the bilinear transformation can be employed for each local frequency window w such that locally the reconstruction is exact. Third, the frequency axis can be adjusted by using $\omega = (2/T) \tan(\bar{\omega}(T/2))$ such that the reconstruction is exact over the full frequency range. Note that this results in non-equidistant frequency points in the ω domain [29].

Summarizing, by applying a suitable Möbius transformation, any available prior knowledge can directly be incorporated into the basis Ψ in the ω domain.

B. Connection to Existing Results

In this section, the presented framework is connected to previous parameterizations in the literature. Applying the Möbius transform $-j$ to the LRMP in (23) results in the well-known continuous-time Takenaka–Malmquist [26] basis. Moreover, if the Möbius transform $-j$ is combined with a bilinear transform, e.g., the Tustin approximation, the discrete-time Takenaka–Malmquist [30] functions are obtained. The generalization in (23) simplifies to the well-known Laguerre functions by taking all $\beta_b \in \mathbb{C}, \mathrm{Re}(\beta) = 0$ such that the rational functions model a system containing first-order real-valued poles. Selecting $\beta_{k+1} = -\bar{\beta}_k \in \mathbb{C}$ such that all complex poles appear in real positive/negative pairs results in the Kautz basis functions. In Fig. 5, the Möbius transformation is used to connect the presented basis to existing results found in the literature [19], [26], [30].

VI. Case Study

In this section, the theory from Section IV with the design guidelines from Section V is applied in a case study: both in a
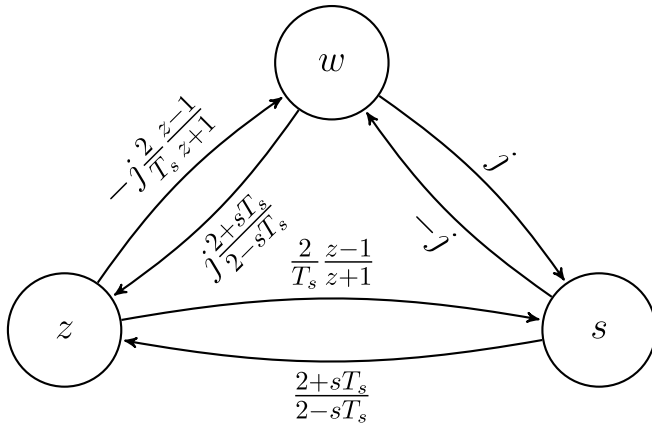
Fig. 5. Diagram indicating the Möbius mapping to connect orthonormal functions in different domains.

simulation study of a mechanical system and an experimental study of a thermal system.

Remark 8: Throughout this section, it is assumed that accurate prior knowledge is available, e.g., through finite-element model (FEM) or initial experiments. In the case of uncertainty in the prior knowledge, mechanisms, such as pole repetition or iterative pole placement, can aid in improving the estimation accuracy. A comprehensive sensitivity analysis toward uncertainty in the prescribed pole locations would provide additional value to the presented method. This sensitivity analysis is outside the scope of the current research.

A. Procedure

In the case study, the following procedure is employed to construct the FRF $\hat{G}$ and variance estimate $\hat{C}_v$.

*Procedure 1 (FRF Identification):* **Require:** Appropriate excitation signal, e.g., white noise or random-phase multisine.

1: **Perform simulation/experiment**
2: **if** Prior knowledge **then** $\beta \leftarrow$ according to Fig. 4
3: **else** $\beta = 0$
4: **end if**
5: **procedure** LRMP($U(k), Y(k), \beta$)
6:     **for** $k \in [0, \ldots, N]$ **do**
7:         Construct (13) to obtain $\hat{\Theta}(k)$
8:         Calculate $\hat{G}(k)$ and/or $\hat{T}(k)$.
9:         Calculate the variance estimate $\hat{C}_v$
10:     **end for**
11: **end procedure**

In this context, an appropriate excitation signal is system dependent, e.g., for a thermal system, an offset to the input is often required since a negative heat flux input is infeasible using conventional actuators.
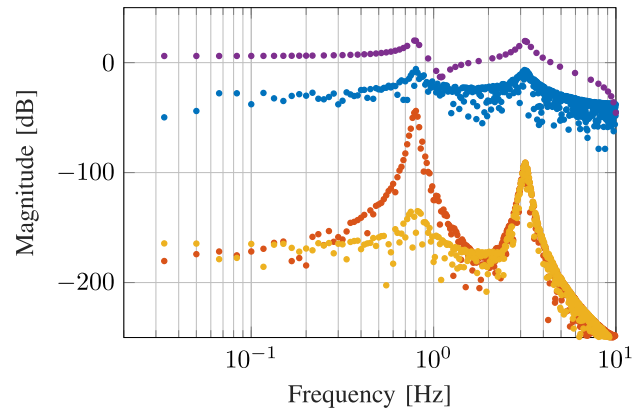
B. Simulation Study: Mechanical System

In this section, the method presented in Section IV is applied to a mechanical system with resonant behavior in a simulation study. The true system is given by
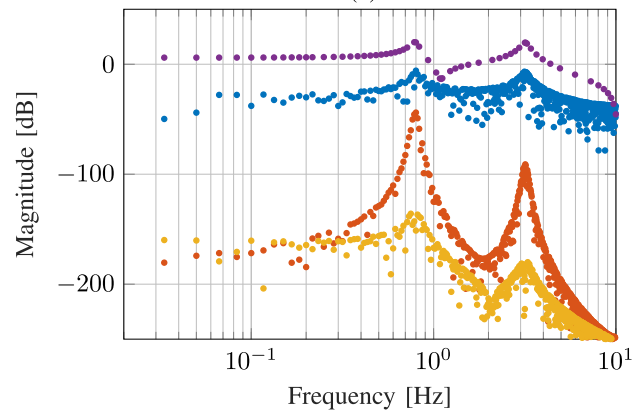
$$G_0(s) = \frac{\Omega_1^2}{s^2 + 2\zeta\Omega_1 + \Omega_1^2} + \frac{\Omega_2^2}{s^2 + 2\zeta\Omega_2 + \Omega_2^2} \quad (27)$$
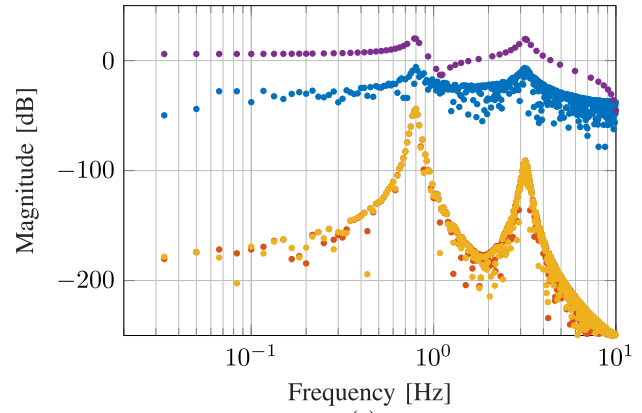
Fig. 6. Reducing the estimation error by incorporating prior knowledge. True plant $G_0(\omega)$ (———) and estimation error $|G_0(\omega) - \hat{G}(\omega)|$ using classical approach (●), LPM (●) and LRMP (●). Here, the LPM is recovered as a special case of the LRMP by selecting $\beta = [0, 0, 0]$, as shown in Fig. 6(a). By incorporating additional prior knowledge, i.e., using the transformations in Fig. 4 to incorporate the system poles γ as pre-scribed poles β, the estimation error is significantly reduced, as shown in Fig. 6(b) and Fig. 6(c). (a) Selecting $\beta = [0, 0, 0]$ recovers the LPM as a special case of the proposed approach. (b) Including prior knowledge on the first resonance peak location by using $\beta = [0.76+0.6i, 0, 0]$. (c) Including both resonance peaks as prior knowledge by including two single complex poles at $\beta = [0.76 + 0.6i, 0.98 + 0.16i, 0]$.

characterized by the natural frequencies $\Omega_1 = 5$ [rad/s] and $\Omega_2 = 4\Omega_1$ and damping coefficient $\zeta = 0.05$. The system $G_0(s)$ is then discretized using zero-order hold with a sample time $T_s = 1/20$ [s] to obtain $G_0(z)$. The dynamics of the
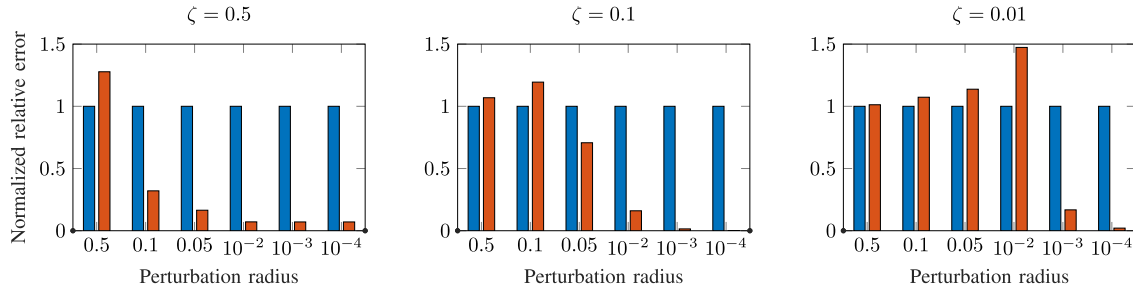
Fig. 7. Maximum relative estimation error for varying magnitudes of complex perturbations in the prior knowledge for systems with different damping coefficients ζ. The results are the median of 100 simulations for each perturbation, comparing the proposed method (■) to the LPM (■). The size of the allowable perturbation is correlated with the amount of damping in the system. The results are normalized with respect to the results obtained with the LPM.

true system is characterized by the system poles that are $\gamma = [0.76 \pm 0.6i, 0.98 \pm 0.16i]$ in discrete time.

The system $G_0(z)$ is excited using two periods of a random-phase multisine of 60 [s] that is defined as

Definition 1:

$$u(n) = \sum_{k=1}^{N} A_k \sin(2\pi f_k n/N + \phi_k) \qquad (28)$$

where n is a specific discrete sample, N is the total number of samples, A_k is the amplitude of the sinusoidal signal at frequency f_k, ϕ_k is a uniformly distributed random phase on $[0, 2\pi)$ such that $\mathbb{E}\{e^{i\phi_k}\} = 0$.

Then, an FRF estimate $\hat{G}_0(\omega)$ is obtained using the classical ETFE approach, the traditional LPM, and the new LRMP approach. The total number of basis functions in the proposed method is $N_b = 3$. Initially, the prescribed poles β are set to 0, i.e., $\beta = [0, 0, 0]$, by doing so the LPM is recovered as a special case of the LRMP. This results in an estimation error, as shown in Fig. 6(a). Here, the LPM and LRMP both obtain a significantly better estimation of $G_0(z)$ when compared to the ETFE. Moreover, it is observed that the LPM and LRMP obtain similar results.

By then applying the LRMP with appropriate prior knowledge, e.g., by employing the transformations in Fig. 4 on the poles α, γ, an improved estimation error is obtained. In Fig. 6(b), the prescribed poles include a single complex pole $\gamma(1)$ at the first resonance of $G_0(z)$. This results in an improved estimation error at the first resonance frequency. By expanding the basis Ψ to include a single complex pole at each resonance, the estimation error is decreased further, as shown in Fig. 6(c).

C. Uncertainty in the Prior Knowledge

The approach presented in this article relies on accurate prior knowledge to reduce the estimation error. In Section VI-B, exact prior knowledge is available on the pole locations. In most practical applications, accurate prior knowledge is available through initial experiments or FEMs. Results of a preliminary investigation into the effect of uncertainty in the prior knowledge on the estimation accuracy of the method proposed in this article are shown in Fig. 7.

The analysis is performed by repeating the procedure of Section VI-B while perturbing the prior knowledge on the

first pole location by complex perturbations within a radius of varying size. As a performance metric, the maximum value of the relative estimation error is compared between the LPM and the proposed method. The median result of 100 simulations for varying perturbation sizes and three different systems with varying damping ratios is shown in Fig. 7. It illustrates that the method proposed in this article is insensitive to large perturbations in the prior knowledge for systems with a large damping ratio. It also shows that for lightly damped systems, increasingly accurate prior knowledge is required to improve the estimation accuracy. For application of the proposed method to very lightly damped systems, a more elaborate sensitivity analysis is recommended and outside the scope of this article.

D. Experimental Study: Thermal System

In this section, an experimental case study on a precision motion system, considered in a thermal control context, is presented.

1) Thermal System: The experimental setup used in this article is shown in Fig. 8(a). A 2-D schematic overview of the setup, including the relevant components and sensor location, is shown in Fig. 8(b). In the original application, the system under test is a high-precision linear motion stage moving in the y-direction, used in optical inspection equipment. In this article, thermal aspects of this setup are investigated. Transient effects in these types of systems are often dominant, and hence, the approach in Section III is expected to be highly applicable.

To isolate the thermal aspects of the system, the linear motor stator is removed, and its rotor, the coils, is maintained. The linear motors are then used as a thermal excitation source by passing a current through the coils, thereby heating them.

2) Transient Response: To facilitate the presentation, a single temperature measurement is used as shown in Fig. 8(b), yielding an SISO system. The system is excited using a random-phase multisine limited to 0.1 Hz, with a peak of 5 W centered around an offset of 5 W, since only heating is possible. Measurements are sampled at $F_s = 1$ [Hz] since the dynamics are predominantly low-frequent. The periodic excitation has a period length of $L = 1$ h, that is repeated $P = 48$ times, yielding a total data set of $F_s L P = 172\,800$ samples. The system response is presented in Fig. 9, and it shows the temperature over a 48-h period.
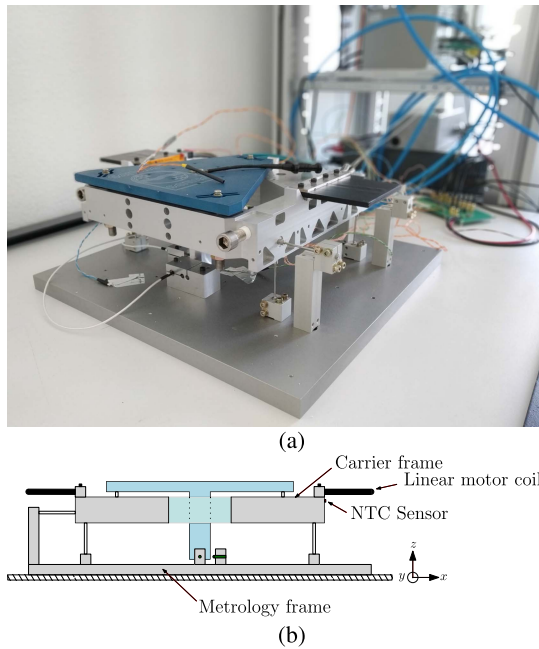
(a)

(b)

Fig. 8. Photograph and illustration of the experimental setup, including the carrier frame and the base plate that is used as a metrology frame. On the illustration, the carrier frame, metrology frame, linear motor coil, and sensor locations are indicated. (a) Photograph of the experimental setup. (b) Illustration of the experimental setup.
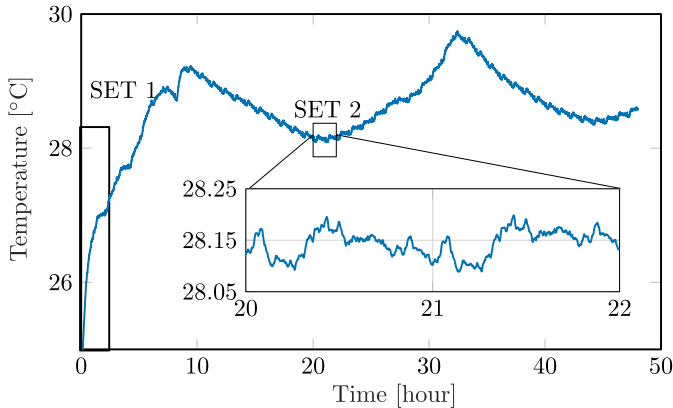

Fig. 9. Temperature response of the experimental setup over a 48-h period. The identification procedure is performed on two separate subrecords, sets 1 and 2, each containing two full periods of the multisine. Set 1 contains the initial response and a strong transient. Conversely, set 2 contains relatively little transient response and is used as a validation data set.

The experimental data as shown in Fig. 9 are separated into two subrecords, i.e., sets 1 and 2. Set 1 contains the first two periods, i.e., 2 h, of the response data that include the strong transient behavior due to the offset in the excitation signal. Set 2 contains the two periods as shown in the magnified plot in Fig. 9, i.e., 2 h starting at hour 20, that contains a minimal amount of transient response and can be used as a validation data set. Furthermore, it is seen that the small and relatively fast dynamic response is superimposed onto a much larger and slower transient response caused by initial excitation and the 24-h, e.g., day/night, cycle of the environment. The prior knowledge that is used in the proposed method is a distribution
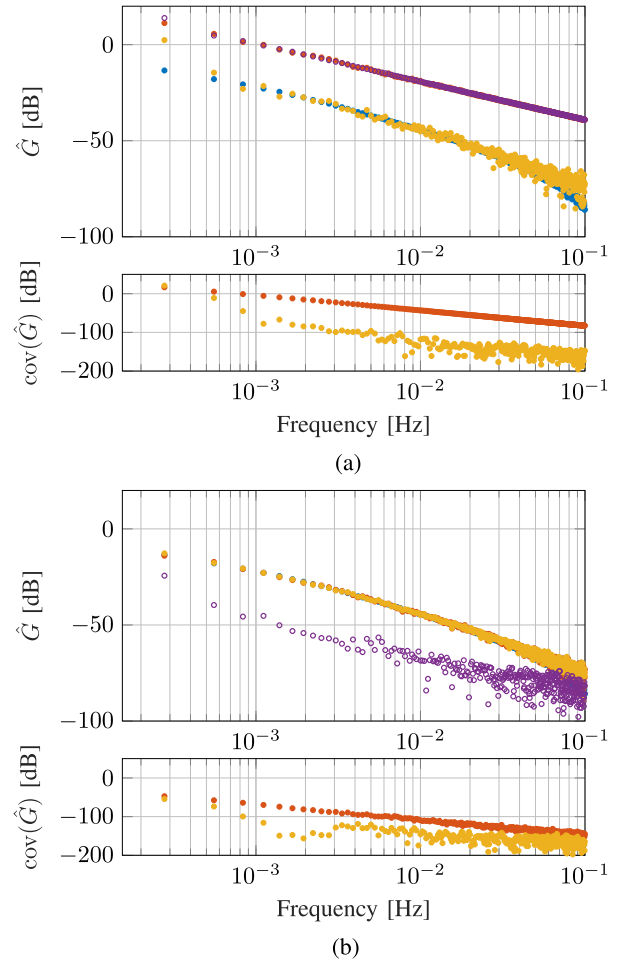

(a)

(b)

Fig. 10. Application of both the traditional approach, the ETFE, and the presented approach, the LRMP, to both subrecords 1 and 2 in Fig. 9. Yielding an FRF $\hat{G}$, transfer function between heater input [W] and temperature output [°C], and corresponding variance $\hat{C}_v$. (a) Application of the ETFE (●) and LRMP (●) to subrecord 1. Interestingly, the ETFE is dominated by the transient contribution. Indeed, the transient T (O) obtained with the LRMP is almost equal to the ETFE. Here, G_0 (●) is shown for validation. Moreover, the variance $\hat{C}_v$ estimation of the ETFE appears to be biased by the transient. (b) To verify the accuracy of the presented LRMP approach, also subrecord 2 is investigated, which is almost transient free. In this case, the LRMP (●) and ETFE (●) obtain almost equal results and approach G_0 (●). The transient T (O) indeed is significantly smaller than in subrecord 1 allowing both the ETFE and LRMP to accurately estimate G_0. However, the variance estimation of the ETFE still appears to be influenced by the residual transient in the estimation, while the LRMP is not.

of $N_b = 3$ poles at $[10^{-4}, 10^{-3}, 10^{-2}]$ Hz. To validate the accuracy of the estimation, a validation FRF G_0 is obtained by averaging over 20 periods between hours 10 and 30. Since the true system is unknown, this FRF G_0 is taken as ground truth where the other methods are compared to.

By applying the classical approach, the ETFE, and the presented method, the LRMP, results shown in Fig. 10 are obtained. The results show the estimated plant $\hat{G}(\omega)$ for both methods and the estimated transient component $\hat{T}(\omega)$. Clearly, the first subrecord contains a strong transient response; therefore, the ETFE yields a biased and poor estimate of G_0. Moreover, the covariance estimate $\text{cov}(\hat{G})$ using the ETFE appears to also be biased by the transient. The presented approach is able to estimate the FRF more accurately since it is

close to G_0. The second subrecord contains significantly less transient contribution, allowing the ETFE to also accurately estimate the FRF. Although the variance $\text{cov}(\hat{G})$ still appears slightly biased since it still deviates from the results obtained through the proposed method. Relying on the second subrecord for FRF estimation requires a significant time investment since an additional 20 h of experimental time is required to obtain the results.

By applying the approach presented in this article, a significant reduction in experimental time is achieved since the FRF can be estimated by measuring 2 h, by using the first subrecord, opposed to 22 h required for the classical approach.

VII. Conclusion

Incorporation of prior knowledge in conjunction with explicit transient estimation leads to improved FRF estimation for a large class of systems, including thermal and mechanical systems. Indeed, the transient response often present in measurements from these systems can cause a biased FRF estimate when employing classical approaches. Recent advancements in FRF identification employ local modeling techniques to estimate and remove these transients from the response. The framework presented in this article enables fast and accurate FRF estimation of a wide class of systems with a reliable quality metric, i.e., covariance expressions. This is achieved by utilizing a unified approach to local parametric modeling. It presents a local rational parameterization while maintaining a closed-form solution by using prescribed poles.

Previous methods, e.g., the LPM, also assume a prior, albeit implicit, by placing the poles at ∞. The method presented in this article leverages the available freedom in the pole locations to increase the estimation accuracy. An approach is provided that leverages appropriate Möbius transformations to incorporate prior knowledge from different domains and applications in the local parameterization. The presented approach yields high-fidelity models that enable the application of advanced design, analysis, and control procedures.

APPENDIX I
APPENDIX//PROOFS

A. Proof to Theorem 1

Proof: Given the results in [26], where it is shown that the continuous-time Takanaka–Malmquist functions, e.g.,

$$B_n(s) = \frac{\sqrt{2\text{Re}\{\alpha_n\}}}{s + \alpha_n} \prod_{l=0}^{k-1} \frac{s - \bar{\alpha}_l}{s + \alpha_l} \tag{29}$$

are orthonormal with respect to

$$\frac{1}{2\pi} \int_{-\infty}^{+\infty} B_n(j\omega)\overline{B_m}(j\omega)d\omega = \begin{cases} 1, & n = m \\ 0, & n \neq m \end{cases} \tag{30}$$

and it suffices to show that $\Psi(\beta, \omega) \equiv B(\alpha, j\omega)$. Given $\alpha = x + jy$ then $\beta = -j\alpha = y - jx$, resulting in

$$\Psi(\beta, \omega) = \sqrt{2x} \frac{-j}{\omega + y - jx} \prod \frac{\omega + y + jx}{\omega + y - jx} \tag{31}$$

$$= \sqrt{2x} \frac{1}{j\omega + x + jy} \prod \frac{j\omega - x + jy}{j\omega + x + jy} \tag{32}$$

$$= \sqrt{2Re\{\alpha\}} \frac{1}{s + \alpha} \prod \frac{s - \bar{\alpha}}{s + \alpha} \tag{33}$$

which concludes the proof. $\square$

B. Proof to Theorem 2

Proof: Given the results in [26], where it is shown that (29) is complete if and only if

$$\sum_{n=1}^{\infty} \frac{\text{Re}\{\alpha_n\}}{1 + |\alpha_n|^2}. \tag{34}$$

It is shown that $\Psi(\beta, \omega) \equiv B(\alpha, j\omega)$. Therefore, it is sufficient to show that (25) is equivalent to (34), where $\beta = -j\alpha$. Since $|\alpha| \equiv |\beta|$ and $\text{Re}\{\alpha\} = \text{Re}\{j\beta\} = -\text{Im}\{\beta\}$, this equivalence is straightforward, which concludes the proof. $\square$

References

[1] T. Oomen, "Advanced motion control for precision mechatronics: Control, identification, and learning of complex systems," *IEEJ J. Ind. Appl.*, vol. 7, no. 2, pp. 127–140, 2018.

[2] A. Karimi and Y. Zhu, "Robust H-infinity controller design using frequency-domain data," in *Proc. 19th IFAC World Congr.*, Cape Town, South Africa, 2014, pp. 4921–4926.

[3] E. Evers, M. van de Wal, and T. Oomen, "Synchronizing decentralized control loops for overall performance enhancement: A youla framework applied to a wafer scanner," *IFAC-PapersOnLine*, vol. 50, no. 1, pp. 10845–10850, Jul. 2017.

[4] R. Pintelon and J. Schoukens, *System Identification: A Frequency Domain Approach*, 2nd ed. Hoboken, NJ, USA: Wiley, 2012.

[5] E. Geerardyn, M. L. D. Lumori, and J. Lataire, "FRF smoothing to improve initial estimates for transfer function identification," *IEEE Trans. Instrum. Meas.*, vol. 64, no. 10, pp. 2838–2847, Oct. 2015.

[6] R. Voorhoeve, A. van Rietschoten, E. Geerardyn, and T. Oomen, "Identification of high-tech motion systems: An active vibration isolation benchmark," *IFAC-PapersOnLine*, vol. 48, no. 28, pp. 1250–1255, 2015.

[7] G. Monteyne, G. Vandersteen, R. Pintelon, and D. Ugryumova, "Transient suppression in FRF measurement: Comparison and analysis of four state-of-the-art methods," *Measurement*, vol. 46, no. 7, pp. 2210–2222, Aug. 2013.

[8] R. Relan, K. Tiels, J.-M. Timmermans, and J. Schoukens, "A local polynomial approach to nonparametric estimation of the best linear approximation of lithium-ion battery from multiple datasets," *IEEE Control Syst. Lett.*, vol. 1, no. 1, pp. 182–187, Jul. 2017.

[9] T. van Keulen, L. Huijben, and T. Oomen, "Identification of control-relevant diesel engine models using a local linear parametric approach," *IFAC-PapersOnLine*, vol. 50, no. 1, pp. 7836–7841, Jul. 2017.

[10] R. Pintelon, J. Schoukens, G. Vandersteen, and K. Barbé, "Estimation of nonparametric noise and FRF models for multivariable systems—Part I: Theory," *Mech. Syst. Signal Process.*, vol. 24, no. 3, pp. 573–595, Apr. 2010.

[11] T. McKelvey and G. Guérin, "Non-parametric frequency response estimation using a local rational model," *IFAC Proc. Volumes*, vol. vol.45, no. 16, pp. 49–54, Jul. 2012.

[12] D. Verbeke and J. Schoukens, "A study of approximation errors in local parametric approaches to frequency response function estimation," *IFAC-PapersOnLine*, vol. 51, no. 15, pp. 814–819, 2018.

[13] E. C. Levy, "Complex-curve fitting," *IRE Trans. Autom. Control*, vol. AC-4, no. 1, pp. 37–43, May 1959.

[14] J. Guo, "Positioning performance enhancement via identication and control of thermal dynamics: A MIMO wafer table case study," M.S. thesis, Dept. Mech. Eng., Eindhoven Univ. Technol., Eindhoven, The Netherlands, May 2014.

[15] R. Relan, K. Tiels, J.-M. Timmermans, and J. Schoukens, "Estimation of best linear approximation from varying operating conditions for the identification of a li-ion battery model," *IFAC-PapersOnLine*, vol. 50, no. 1, pp. 4739–4744, 2017.

[16] D. Peumans, C. Busschots, G. Vandersteen, and R. Pintelon, "Improved FRF measurements of lightly damped systems using local rational models," *IEEE Trans. Instrum. Meas.*, vol. 67, no. 7, pp. 1749–1759, Jul. 2018.

[17] D. Peumans, A. De Vestel, C. Busschots, Y. Rolain, R. Pintelon, and G. Vandersteen, "Accurate estimation of the non-parametric FRF of lightly-damped mechanical systems using arbitrary excitations," *Mech. Syst. Signal Process.*, vol. 130, pp. 545–564, Sep. 2019.

[18] D. K. de Vries and P. M. J. Van den Hof, "Frequency domain identification with generalized orthonormal basis functions," *IEEE Trans. Autom. Control*, vol. 43, no. 5, pp. 656–669, May 1998.

[19] B. Ninness and F. Gustafsson, "A unifying construction of orthonormal bases for system identification," *IEEE Trans. Autom. Control*, vol. 42, no. 4, pp. 515–521, Apr. 1997.

[20] P. S. C. Heuberger, P. M. J. van den Hof, and B. Wahlberg, Eds., *Modelling and Identification with Rational Orthogonal Basis Functions*. London, U.K.: Springer, 2005.

[21] E. Evers, B. de Jager, and T. Oomen, "Improved local rational method by incorporating system knowledge: With application to mechanical and thermal dynamical systems," *IFAC-PapersOnLine*, vol. 51, no. 15, pp. 808–813, 2018.

[22] J. Schoukens, G. Vandersteen, Y. Rolain, and R. Pintelon, "Frequency response function measurements using concatenated subrecords with arbitrary length," *IEEE Trans. Instrum. Meas.*, vol. 61, no. 10, pp. 2682–2688, Oct. 2012.

[23] E. Geerardyn, "Development of user-friendly system identification techniques," Ph.D. dissertation, Dept. Fundam. Electr. Instrum., Vrije Universiteit Brussel, Brussels, Belgium, 2016.

[24] R. Voorhoeve, A. van der Maas, and T. Oomen, "Non-parametric identification of multivariable systems: A local rational modeling approach with application to a vibration isolation benchmark," *Mech. Syst. Signal Process.*, vol. 105, pp. 129–152, May 2018.

[25] B. Ninness, S. Gibson, and S. Weller, "Practical aspects of using orthonormal system parameterisations in estimation problems," *IFAC Proc. Volumes*, vol. 33, no. 15, pp. 463–468, Jun. 2000.

[26] H. Akçay and B. Ninness, "Orthonormal basis functions for modelling continuous-time systems," *Signal Process.*, vol. 77, no. 3, pp. 261–274, Sep. 1999.

[27] R. M. A. van Herpen, "Identification for control of complex motion systems : Optimal numerical conditioning using data-dependent polynomial bases," Ph.D. dissertation, Dept. Mech. Eng., Eindhoven Univ. Technol., Eindhoven, Netherlands, 2014.

[28] B. Ninness, H. Hjalmarsson, and F. Gustafsson, "The fundamental role of general orthonormal bases in system identification," *IEEE Trans. Autom. Control*, vol. 44, no. 7, pp. 1384–1406, Jul. 1999.

[29] C. H. Houpis and G. B. Lamont, *Digital Control Systems: Theory, Hardware, Software*, 2nd ed. New York, NY, USA: McGraw-Hill, 1992.

[30] S. Takenaka, "On the orthogonal functions and a new formula of interpolation," *Jpn. J. Math., Trans. Abstr.*, vol. 2, no. 0, pp. 129–145, 1925.

Enzo Evers received the M.Sc. *(cum laude)*, and Ph.D. degrees in mechanical engineering from the Eindhoven University of Technology, Eindhoven, The Netherlands, in 2016 and 2021, respectively. His Ph.D. thesis was centered on advanced identification and control for thermomechanical systems.

He has contributions in the areas of modeling, actuation design, and control. He is currently a University Researcher with the Control Systems Technology Group, Department of Mechanical Engineering, Eindhoven University of Technology.

Bram de Jager received the M.Sc. degree in mechanical engineering from the Delft University of Technology, Delft, The Netherlands, and the Ph.D. degree from the Eindhoven University of Technology, Eindhoven, The Netherlands.

He was with the Delft University of Technology and Stork Boilers BV, Hengelo, The Netherlands. He is currently with the Eindhoven University of Technology. His research interests include robust control of (nonlinear) mechanical systems, integrated control and structural design, control of fluidic systems, and control structure design and applications of (nonlinear) optimal control.

Tom Oomen (Senior Member, IEEE) received the M.Sc. *(cum laude)* and Ph.D. degrees from the Eindhoven University of Technology, Eindhoven, The Netherlands, in 2005 and 2010, respectively.

He held visiting positions at KTH, Stockholm, Sweden, and The University of Newcastle, Callaghan, NSW, Australia. He is currently an Associate Professor with the Department of Mechanical Engineering, Eindhoven University of Technology, Eindhoven, The Netherlands. His research interests are in the field of data-driven modeling, learning, and control, with applications in precision mechatronics.

Dr. Oomen is a member of the Eindhoven Young Academy of Engineering. He was a recipient of the Corus Young Talent Graduation Award, the IFAC 2019 TC 4.2 Mechatronics Young Research Award, the 2015 IEEE TRANSACTIONS ON CONTROL SYSTEMS TECHNOLOGY Outstanding Paper Award, the 2017 IFAC Mechatronics Best Paper Award, the 2019 IEEJ Journal of Industry Applications Best Paper Award, and the Veni and Vidi Personal Grant. He is also an Associate Editor of the IEEE CONTROL SYSTEMS LETTERS (L-CSS), *IFAC Mechatronics*, and IEEE TRANSACTIONS ON CONTROL SYSTEMS TECHNOLOGY.